SOILS AND FOUNDATIONS Vol. 39, No. 1, 31-41, Feb. 1999
Japanese Geotechnical Society

ENGINEERING PROPERTIES OF SOIL STABILIZED BY FERRUM LIME AND USED FOR THE APPLICATION OF ROAD BASE

MASASHI KAMON[i], HUANDA GU[ii] and TAKESHI KATSUMI[iii]

ABSTRACT

In this paper, the behavior of soil stabilized by ferrum lime, a mixture composed of ferric oxide (Fe_2O_3) and hydrated lime ($Ca(OH)_2$), is investigated in order to assess the engineering properties of the stabilized soil for its application to road construction. The aptitude of the ferrum-lime stabilized soil as road base material is evaluated according to the static compressive, static flexural, and dynamic resilient properties of materials obtained from laboratory tests. The ferric oxide promotes an increase in both compressive strength and the stiffness of the stabilized soil. Resilient modulus M_r, a parameter expressing the material behavior under dynamic cyclic loading, depends on the deviator stress and the mean principal stress. Under lower deviator stress and mean principal stress conditions, the M_r of the ferrum-lime stabilized soil has a higher value than that of the hydrated-lime stabilized soil. However, the difference in resilient modulus M_r between the two types of stabilized soils may not be distinct with increases in the deviator stress and the mean principal stress. In addition, the dependence of resilient modulus M_r on the static strength of the ferrum-lime stabilized soil can be observed. Fracture surface energy γ_s, a parameter which indicates the resistance ability of a material to cracks, is related to the deflection at failure, but hardly depends on the flexural strength. The γ_s has almost the same values for both type of stabilized soils. According to test results, ferric oxide can improve the durability of pavement when it is used as a stabilizer for lime stabilized soil.

Key words: compressive strength, cyclic load, ferric oxide, flexural strength, fracture surface energy, hydrated lime, resilient modulus, road base, stabilized soil (**IGC**: D10)

INTRODUCTION

In recent years, the problem of the fatigue failure of pavement has become more serious, one of the important factors being the weakness of road base due to heavy loads of traffic. Strengthening the road base with a stabilized material is considered to be an important method for improving pavement durability.

Ferrum lime, a mixture of ferric oxide and hydrated lime, has been used as a stabilizer for road base since the 1960s, especially in the western part of Japan. Even if pavement containing the ferrum-lime stabilized soil is subjected to heavy traffic loads over a long period of time, fatigue failures such as rutting and cracks are rare (Abe, 1993). The ferric oxide used in the ferrum lime is a by-product of iron smelting. Since the use of waste products as construction materials has become an ever-increasing concern in regard to environmental protection, fly ash, for instance, which is mixed with fine-grained material and used as road base material, has been evaluated (Lee and Fishman, 1993). Therefore, using ferrum lime as a stabilizer for road base can be expected to improve the durability of pavement together with the use of waste products.

The mechanical properties of stabilized soils used as road base materials may be affected by loading conditions, the stabilizer content, the curing time, the curing pattern, temperature, and so on. Boniface and Obi (1972) examined the resilient and the residual deformation properties of cement-stabilized soil under dynamic loading conditions. Sauer and Weiner (1978) investigated the effects of loading conditions and additive contents on the resilient deformation characteristics of lime-stabilized soil subjected to dynamic loads. The effects of temperature and water content on resilient modulus M_r were explored by Mamlouk and Wood. (1981) and Jin *et al.* (1994). Furthermore, there may be a correlation between the dynamic mechanical properties and static mechanical properties such as static compressive properties, CBR, cohesion C, friction angle ϕ, and so on (Thompson *et al.*,

i) Professor, Disaster Prevention Research Institute, Kyoto University, Gokasho, Uji, Kyoto-611-0011. (Telephone: 0774-38-4090, Facsimile: 0774-38-4030, e-mail: kamon@geotech.dpri.kyoto-u.ac.jp).
ii) Graduate Student, Department of Civil Engineering, Kyoto University, Yoshida-Honmachi, Kyoto-606-8317.
iii) Research Associate, Disaster Prevention Research Institute, Kyoto University, Gokasho, Uji, Kyoto-611-0011.
Manuscript was received for review on September 26, 1997.
Written discussions on this paper should be submitted before September 1, 1999 to the Japanese Geotechnical Society, Sugayama Bldg., 4F, Kanda Awaji-cho, 2-23, Chiyoda-ku, Tokyo 101-0063, Japan. Upon request the closing date may be extended one month.

1979; Zaman et al., 1994). To evaluate the durability of pavement against fractures, George (1970) measured the critical strain energy release rates by means of beam tests on cement-stabilized soil. Similarly, Blight (1973) estimated the fractures to pavement on lime-stabilized soil and, Khedr (1986) derived a theoretical approach for predicting the permanent deformation in pavement layers based on the fracture mechanics approach by Griffith.

Although substantial results are in evidence, a mechanism dealing with the ability of ferric oxide contained in ferrum lime to improve the durability of pavement has not been clarified. The objectives of this paper are to evaluate the performance of ferrum-lime stabilized soil as road base material and to define the mechanism concerning its ability to improve the durability of pavement with the ferric oxide contained in ferrum lime. The current investigation focuses on the mechanical properties of materials under static and dynamic loading conditions, and by making a comparison with hydrated-lime stabilized soil, the effect of ferric oxide on the mechanical properties and the durability of the stabilized soil can be appraised. Future research should address the micro organization of stabilized soil by electron microscope to examine the connection between the mechanical properties of the materials and the crystal composition among soil grains.

MATERIALS AND TEST PROCEDURES

Material and Sample Preparation

The material used for the stabilization in this study was decomposed granite soil, sampled in the town of Nakagawa in Fukuoka Prefecture. The material properties of the soil are summarized in Table 1.

The solidification agents are ferrum lime and hydrated lime. Ferrum lime is a mixture of hydrated lime ($Ca(OH)_2$) and ferric oxide (Fe_2O_3) with a mixing ratio of 3:1. The composition of the ferric oxide is shown in Table 2.

The samples for unconfined compression and dynamic triaxial cyclic tests were made by a compacting method with mold (ϕ5.0 cm × 10 cm) on the basis of JIS A 1210, but the compacting energy was in light of the unconfined compressive test standards of the Japan Cement Association with compacting efforts of 10, 20, 20 and 40 × 4 layers. The wet density of the samples was about 2.10 g/cm^3. Beam specimens (16 cm × 4 cm × 4 cm) for the bending tests were also made by compacting with the same value of wet density as that for the specimens in the unconfined compression tests.

All of the test samples were cured in water at a temperature of 20°C. The stabilized material, additive content, and curing time of the test samples are all presented in Table 3.

Table 1. Material properties of soil

Particle density (g/cm^3)	2.64
Maximum grain size (mm)	4.75
D_{50} (mm)	0.85
Content of silt and clay (%)	15.1
Optimum moisture content (%)	11.9
Maximum dry density (g/cm^3)	1.87
Unconfined compressive strength (kPa)	134
CBR (%)	16.5

Table 2. Composition of ferric oxide

Composition	Fe_2O_3	Al_2O_3	SiO_2	FeO	others
Content (%)	94.92	1.02	0.48	0.27	3.31

Static Compressive and Flexural Tests

The unconfined compressive tests were carried out according to JIS A 1216. The bending tests were based on JIS A 1106 but some modifications were adopted so as to agree with a control system of the test device. A simply supported beam specimen was subjected to a center point load with a controlled-deflection (strain) ratio of 1.0 mm/min. The results of the bending tests called flexural strength, were expressed in the form of the following equation (JIS R 5201):

$$\sigma_b = 2.293 \times 10^{-2} P \qquad (1)$$

where σ_b are the magnitudes of flexural strength (MPa) and P is the largest loading force during testing (kgf).

To measure the fracture surface area of the broken specimens after the bending tests, the Laser Roughness Measurer was used. Employing this instrument, the laser

Table 3. Laboratory testing cases

Case	Solidification	Mixing content (%)	Testing projects	Curing time (days)
1	Ferrum lime	4	Unconfined compressive, bending	7
2	Ferrum lime	7	Unconfined compressive, bending	7
3	Ferrum lime	10	Unconfined compressive, bending	7
4	Ferrum lime	4	Unconfined compressive, bending, dynamic triaxial	28
5	Ferrum lime	7	Unconfined compressive, bending, dynamic triaxial	28
6	Ferrum lime	10	Unconfined compressive, bending, dynamic triaxial	28
7	Ferrum lime	4	Unconfined compressive, bending	90
8	Ferrum lime	7	Unconfined compressive, bending	90
9	Ferrum lime	10	Unconfined compressive, bending	90
10	Hydrated lime	7	Unconfined compressive, bending, dynamic triaxial	28

Table 4. Loading conditions of cyclic triaxial tests

Loading wave	Sine wave
Number of loading cycles	30,000
Loading condition	0.1 (s) loading, 0.9 (s) rest
Deviator stress (kPa)	58.9~618.0
Mean principal stress (kPa)	98.1, 196.2, 294.3

beam scanned the fracture surface of the broken specimens, the height of the measured points on the fracture surface were recorded by a computer, and from these data the fracture surface area of the broken specimens could be calculated. In measuring, the scanning intermission was set at 1.0 mm.

Dynamic Cyclic Triaxial Test

In view of the dependence of the resilient modulus on the subjected stress, the stress application was modified during dynamic triaxial cyclic tests. The three levels of mean principal stress were 98.1 kPa, 196.2 kPa, and 294.3 kPa. The deviator stress and the confining pressure were modified during the tests to maintain a certain mean principal stress level (Nishi and Yoshida, 1993). The loading conditions in the dynamic triaxial cyclic tests are shown in Table 4.

The testing procedures, in accordance with Nishi (1981), are described below. The test samples were saturated using the vacuum saturation container. The saturated samples were set in triaxial cells, and were consolidated isotropically with the pressure used in the cyclic triaxial tests. Cyclic loading was carried out with the determined stress level until the residual deformation of the tested samples was almost fixed. The number of cyclic loadings was 30,000 in this study. The deviator stress and confining pressure were modified gradually while maintaining a certain mean principal stress.

STATIC PROPERTIES OF FERRUM LIME STABILIZED SOIL

Static Compressive Properties

The unconfined compressive strength increases with an increase in the curing time according to the information in Fig. 1. Simultaneously, a tendency can be observed from this figure, whereby the unconfined compressive strength augments with an increase in the ferrum lime content from 4% to 7%, but the increase is not significant when the ferrum lime content exceeds 7%, in spite of changing the curing time. This appearance may be explained as follows. The strength development of stabilized soils depends primarily on the chemical reaction products and reaction rate during stabilization proceeding, and the chemical reaction products and the reaction rate are related to the reactive elements or ions from stabilizer and soil. Generally, the main chemical reactions in lime stabilized soil are cement hydration reaction and pozzolanic reaction. Through these chemical reactions, several types of hydroxides as well as calcium carbonate $CaCO_3$ are produced. These chemical reaction products fill up the void between soil particles and reinforce the connections among soil particles; this will lead to the strength development of stabilized soil. Comparing ferrum lime with hydrated lime, the content of ferric oxide of the former is richer than the latter. Matsuo and Kamon (1977) reported that the cementation of iron ions oxidation leads to the granular structure of clay particles and reinforces the connections among soil particles. Furthermore, through hydration, the ferric oxide Fe_2O_3 contained in stabilized soil combines with other reactive element such as Ca^{2+} to form Fe series hydroxides. Therefore, adding ferric oxide to stabilized soil plays an active role in the production of chemical reaction products and the reinforcement of connections between soil particles. Finally, the result will lead to the strength improvement of stabilized soil. Since the production of chemical reaction products is also associated with the amount of clay mineral contained in the soil, the results shown in Fig. 1 indicate that the chemical reaction products may not increase continuously in spite of the content of ferrum lime rising over 7% because of the limited amount of clay mineral contained in the decomposed granite soil.

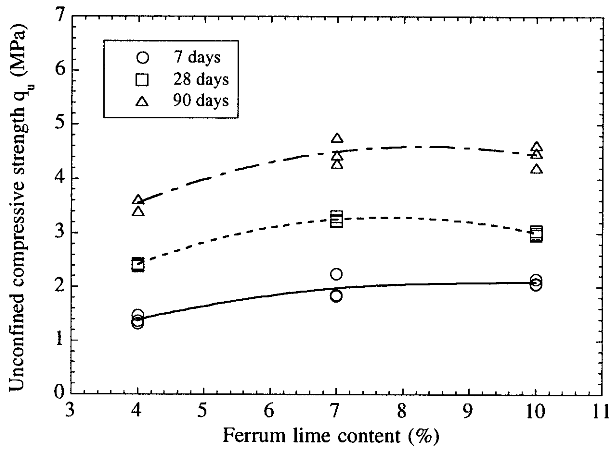

Fig. 1. Strength characteristic of soil stabilized by ferrum lime

As shown in Fig. 2, static modulus E_{50} increases with an increase in the curing time. Such a tendency is observed for specimens with a 7% or 10% ferrum lime content. For specimens with a 4% ferrum lime content, static modulus E_{50} shows quite a small increment after 28 days of curing. Similar to the unconfined compressive strength, the increment of static modulus E_{50} is not distinct in spite of increasing the ferrum lime content from 7% to 10%.

Based on the above-mentioned results, it is unnecessary to use a ferrum lime content over 7% to promote the compressive strength of ferrum-lime stabilized soil.

The data presented in Fig. 3 exhibit a linear relationship between static modulus E_{50} and unconfined compressive strength q_u.

$$E_{50}=210.47q_u \tag{2}$$

where E_{50} is the static modulus (MPa) and q_u is the unconfined compressive strength (MPa).

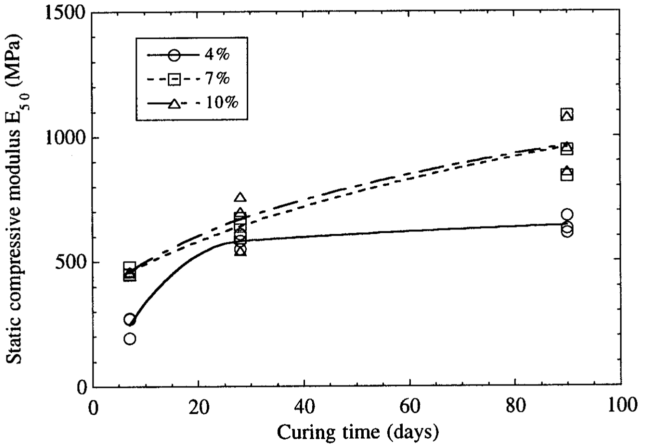

Fig. 2. Variation in static compressive modulus E_{50} with increase in curing time

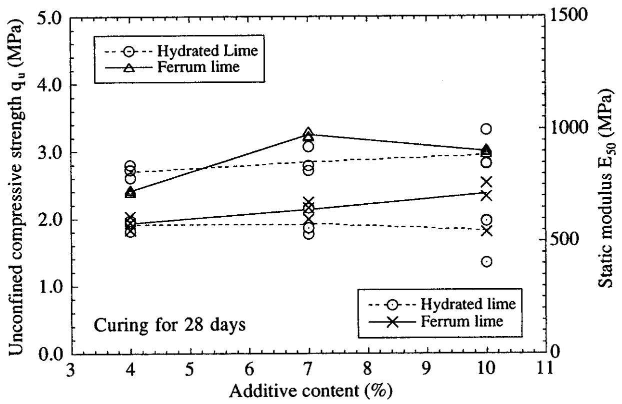

Fig. 4. Unconfined compressive strength q_u and static modulus E_{50} versus additive content

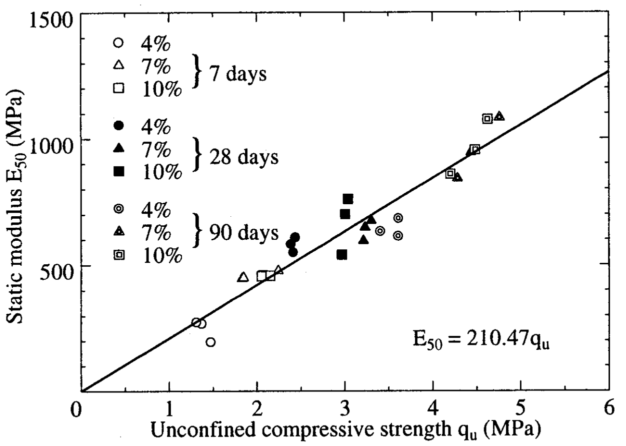

Fig. 3. Static modulus E_{50} versus compressive strength q_u

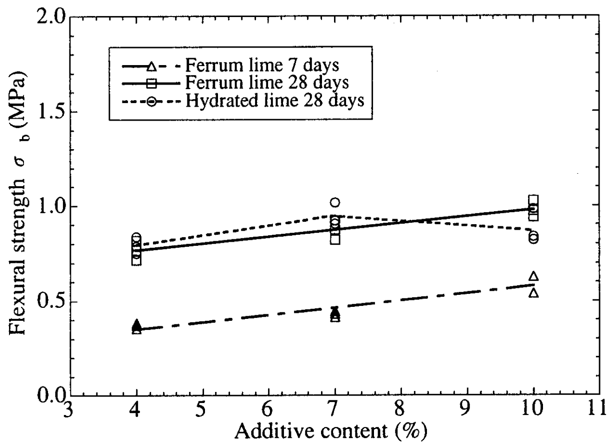

Fig. 5. Variation in flexural strength σ_b with increase in additive content for ferrum lime and hydrated lime stabilized soils

Comparing the ferrum lime with the hydrated lime as a stabilizing agent in Fig. 4, the ferrum-lime stabilized soil can perform comparably or better in unconfined compressive strength as opposed to the hydrated-lime stabilized soil if the ferrum lime content exceeds 4%. The static modulus E_{50} for the two types of stabilized soils has almost the same value at a 4% stabilizer content. However, the E_{50} of the ferrum-lime stabilized soil has an incremental tendency. Inversely, the E_{50} of the hydrated-lime stabilized soil may tend to decrease if the stabilizer content is increased. As a result, the difference in E_{50} between the two kinds of stabilized soils tends to increase gradually with an increase in the stabilizer content of the soils.

Based on the above results, adding ferric oxide to hydrated lime can promote the compressive strength of the stabilized soil.

Static Flexural Properties and the Relationship with Unconfined Compressive Properties

Figure 5 shows the flexural strength results for the specimens stabilized by ferrum lime and hydrated lime. The flexural strength of the ferrum-lime stabilized soil increases with an increase in the ferrum lime content and the curing time. Compared to the results of hydrated-lime stabilized soil, the difference in flexural strength between the two types of stabilized soils is not distinct. However, the flexural strength of the hydrated lime stabilized soil seems to start to decrease if a hydrated lime content of over 7% is added.

Similar to E_{50} in the unconfined compressive tests, E_b was defined as the slope of the load-deflection curve in bending tests to evaluate the bending rigidity of the samples. According to Fig. 6, the E_b of the stabilized soils rises with an increase in the stabilizer content and the curing time. The E_b of the hydrated-lime stabilized soil shows a lower value as opposed to the ferrum-lime stabilized soil if a stabilizer content of over 4% is added. The failure deflection of ferrum-lime stabilized soil specimens seems to decrease slightly with an increase in the ferrum lime content. Based on this fact, the brittleness of the ferrum-lime stabilized soil may be increased by increasing the ferrum lime content in the soil. By plotting the data of the hydrated-lime stabilized soil in the same figure, the hydrated-lime stabilized soil has a larger failure deflec-

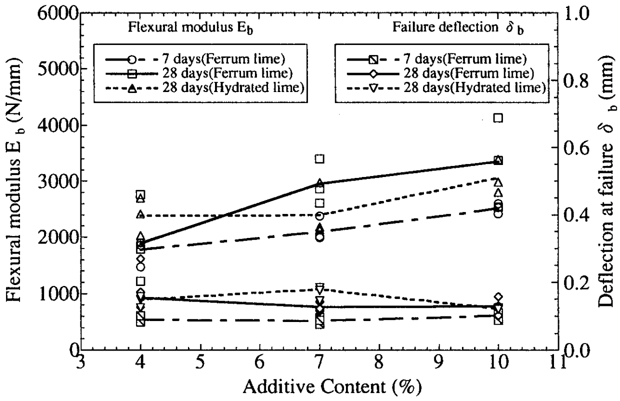

Fig. 6. Variation in flexural modulus E_b and deflection at failure with increase in additive content for ferrum lime and hydrated lime stabilized soils

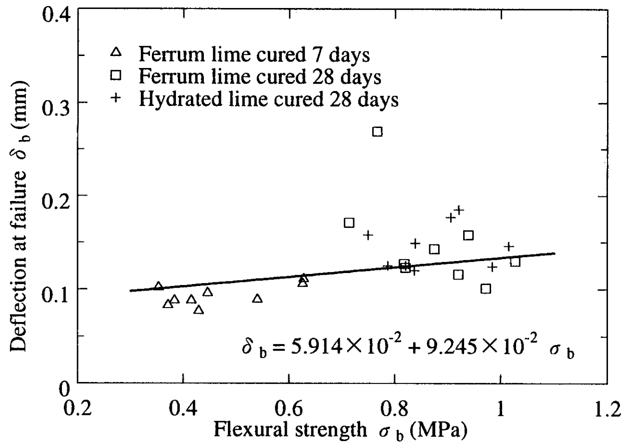

Fig. 8. Variation of failure deflection with flexural strength increase

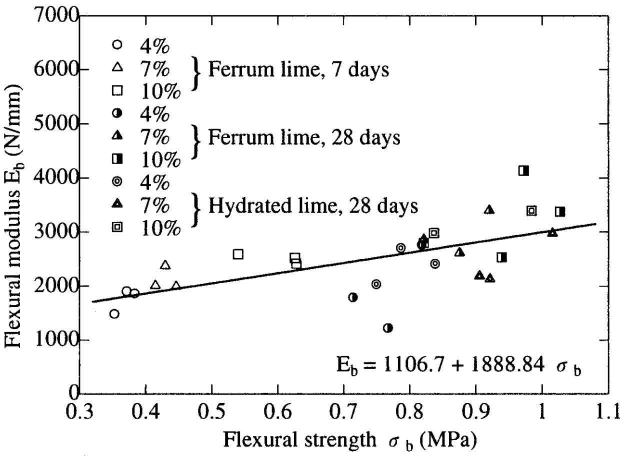

Fig. 7. Flexural modulus E_b versus flexural strength σ_b

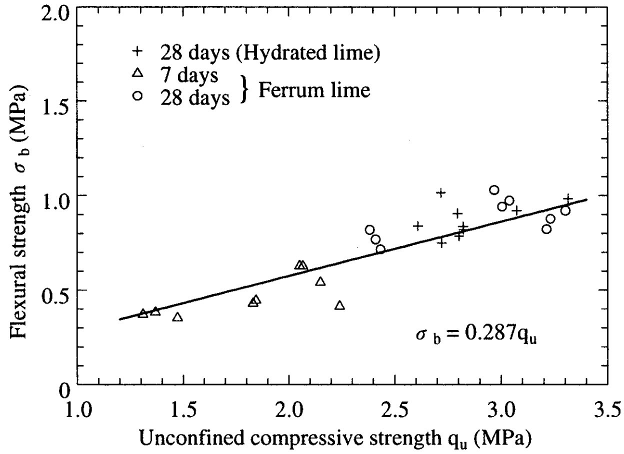

Fig. 9. Unconfined compressive strength versus flexural strength for two kinds of stabilized soils

tion against the ferrum-lime stabilized soil at an additive content of 7%. However, the difference in the failure deflection between the two types of stabilized soils is not clear at additive contents of 4% and 10%.

As shown in Figs. 7, 8 and 9, flexural modulus E_b, deflection at failure δ_b, and unconfined compressive strength q_u all show an incremental trend with an increase in flexural strength σ_b. The correlation between unconfined compressive strength q_u and flexural strength σ_b can be expressed approximately by following linear equation as

$$\sigma_b = 0.287 q_u \tag{3}$$

where σ_b is the flexural strength and q_u is the unconfined compressive strength.

The flexural failure deflection seems to decrease with an increase in the compressive failure strain based on Fig. 10. According to the analysis in the next section, therefore, the material with the larger flexural deflection at failure may possess a higher durability to bending, so to speak and the samples with a lower compressive failure strain may also have a greater ability to resist flexural failure.

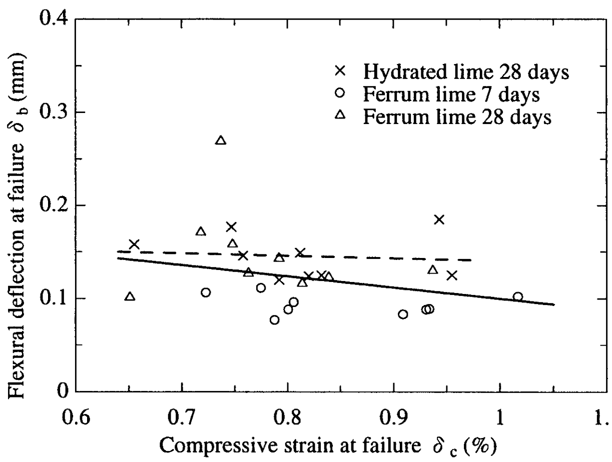

Fig. 10. The flexural failure deflection versus compressive failure strain

Fracture Surface Energy Analyses

The fatigue life of road base is related to the flexural strength of the material (George, 1970). To assess the correlation between the fracture of road base materials and

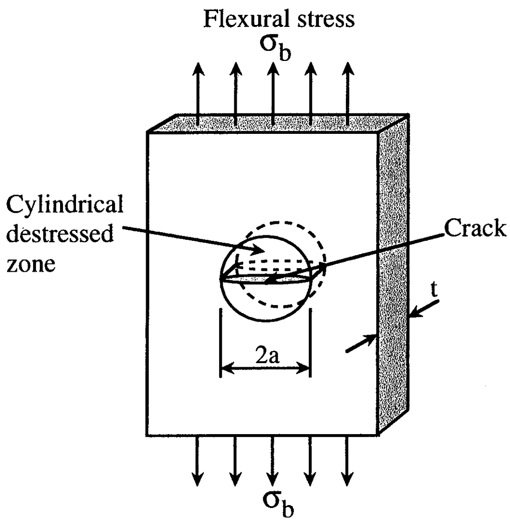

Fig. 11. Through-thickness crack in large plate

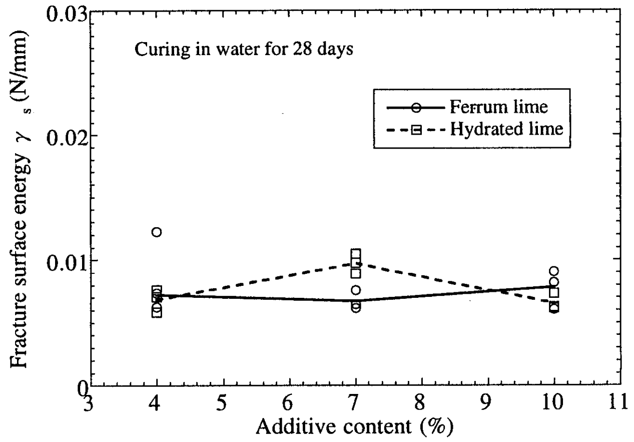

Fig. 12. Fracture surface energy γ_s versus additive content

the flexural strength, Griffith used the model shown in Fig. 11 to establish the conjunction between surface energy γ_s and fracture size a (Blight, 1973). Following this model, surface energy γ_s was estimated to be the product of the total crack surface area ($2a\times 2\times t$); surface energy γ_s has units of energy per unit area. Based on the case of an infinitely large plate containing an elliptical crack, the decrease in stored elastic energy of the cracked plate is $(\pi\sigma^2a^2t)/E$. Thus, the change in elastic energy of the plate associated with the introduction of a crack may be supplied by

$$U-U_0=4at\gamma_s-\frac{\pi\sigma^2a^2t}{E} \tag{4}$$

where U is the elastic energy of a body with cracks, U_0 is the initial elastic energy of a body without cracks, σ is the applied stress, a is one half of the crack length, t is the thickness of the plate, E is the modulus of elasticity, and γ_s is the surface energy. A crack can only spread if the elastic energy is a maximum to a. For this, differentiate the U with respect to the crack length a and set equal to zero,

$$\frac{\partial U}{\partial a}=4t\gamma_s-\frac{2\pi\sigma^2at}{E}=0 \tag{5}$$

Therefore

$$\frac{\sigma^2a}{2E}=\frac{\gamma_s}{\pi} \tag{6}$$

represents the equilibrium condition. From Eq. (5), the basic form of the equation is

$$\sigma=cons\tan t\times\left(\frac{E\gamma_s}{a}\right)^{1/2} \tag{7}$$

Griffith's equation was elected with a perfectly elastic material. In general, the deformation at failure for most materials may include on elastic component and a plastic component. In this case, the equation for tensile strength will be shown as follows (Khedr, 1986):

$$\sigma=cons\tan t\times\left(\frac{E(\gamma_e+\gamma_p)}{a}\right)^{1/2} \tag{8}$$

where γ_e is the elastic work, γ_p is the plastic work, and $\gamma_s=\gamma_e+\gamma_p$.

According to the bending test results, the load-deflection curve is close to a straight line before failure. It can be assumed that the ductility of the specimens is not great before failure. Based on this fact, surface energy γ_s may be approximately equal to elastic surface energy γ_e.

As a parameter of materials, the higher the value of γ_s for a material, the greater its resistance to fractures. Surface energy γ_s can be evaluated by equating the work performed by the applied load to produce fractures to the area of the fracture surface produced. The work performed by the applied load can be obtained from the area under the load-deflection curve and area of the fracture surface may be achieved with a Laser Roughness Measurer. Therefore, surface energy γ_s may be defined as follows:

$$\gamma_s=\frac{A_{w,\delta}}{A_f} \tag{9}$$

where $A_{w,\delta}$ is the area under the load-deflection curve and A_f is the area of the fracture surface.

The results for ferrum-lime and hydrated lime stabilized soils are shown in Fig. 12. The ferrum lime content has surprisingly little influence on the fracture surface energy for ferrum lime stabilized soil. This fact may be explained by bending tests. The fracture deflection starts to decrease with an increase in the ferrum lime content in spite of the increase in flexural strength. As a result, the load-deflection energy hardly changes even after increasing the ferrum lime content. The surface energy for hydrated lime stabilized soil increases with an increase in the hydrated lime content from 4% to 7%. However, it will begin to decrease if the hydrated lime content exceeds 7%. The reason is that both the flexural strength and the fracture deflection tend to decrease when the hydrated lime content exceeds 7%.

If area ratio S_a is defined as the ratio of the fracture surface area to the section area of the specimens, then the S_a is around the value of 1.09, although fracture surface energy γ_s varies from 6×10^{-3} (N/mm) to 12×10^{-3} (N/mm) as shown in Fig. 13. Therefore, it may be concluded that the area of the fracture surface has an approximately 9% increment against the section area of the specimens.

In investigating the correlations between fracture surface energy γ_s and flexural strength as well as the modulus, fracture surface energy γ_s seems to have a low dependency on the flexural strength for both ferrum-lime and hydrated-lime stabilized soils, based on Fig. 14. However, fracture surface energy γ_s seems to depend on the modulus according to Fig. 15. Fracture surface energy γ_s decreases with an increase in both static modulus E_{50} and flexural modulus E_b. Notably, this phenomenon seems to be remarkable even for the relation between fracture surface energy γ_s and flexural modulus E_b.

In Fig. 16, the correlation between fracture surface energy γ_s and failure deflection δ_d is investigated. Fracture surface energy γ_s has a strong dependence on failure deflection δ_d, and it increases with an increase in failure deflection δ_d. Furthermore, this relation can be expressed approximately as follows:

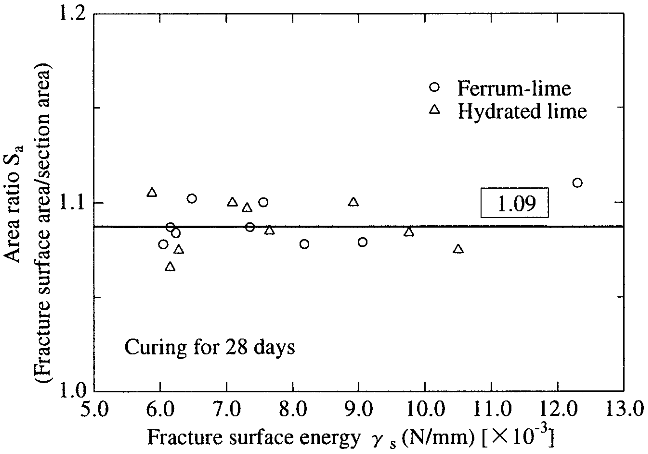

Fig. 13. Area ratio S_a versus fracture surface energy γ_s

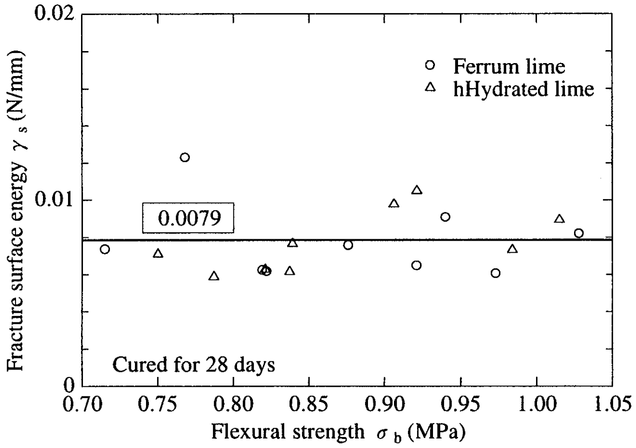

Fig. 14. Fracture surface energy γ_s versus flexural strength σ_b

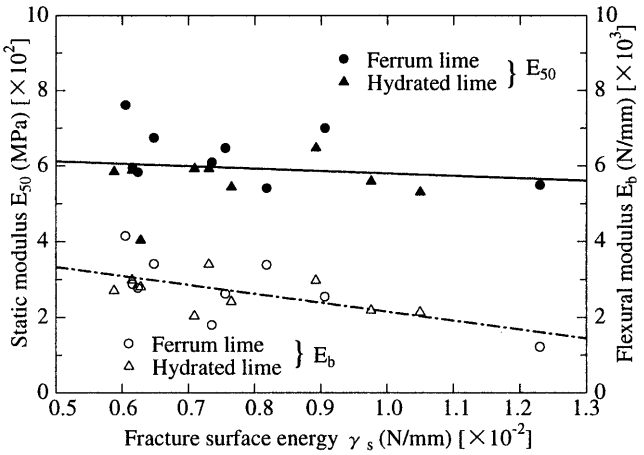

Fig. 15. Relationship between fracture surface energy and static modulus E_{50} or flexural modulus E_b

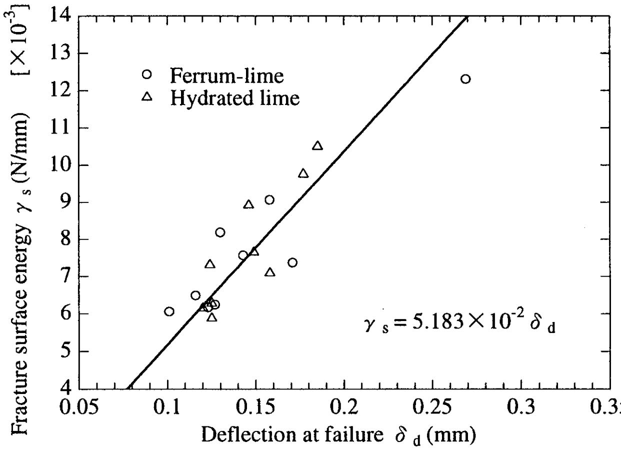

Fig. 16. Deflection at failure versus fracture surface energy for ferrum lime and hydrated lime stabilized soils

$$\gamma_s = 5.183\times10^{-2}\delta_b. \tag{10}$$

According to the above-mentioned results, increasing modulus E_{50} or E_b may lead to a reduction in fracture surface energy γ_s. A higher failure deflection means greater toughness, and the materials with greater toughness may have a higher capacity to resist fractures. In conclusion, only increasing the strength or the stiffness of the materials may be somewhat effective in improving the resistibility against fractures. By improving the toughness of the materials, they may have a larger value of deflection at failure and a larger fracture surface energy γ_s, and the resistibility to cracks can be clearly improved. The difference in resistibility to cracks between hydrated lime stabilized soil and ferrum lime stabilized soil is not clear according to the above results.

RESILIENT CHARACTERISTICS OF FERRUM-LIME STABILIZED SOIL

Determination of the Resilient Modulus

The resilient modulus is generally used for evaluating the behavior of pavement under traffic loading. The resilient modulus M_r of materials in cyclic loading tests is defined by the following form (Brown, 1996):

$$M_r=\frac{\sigma_d}{\varepsilon_a} \tag{11}$$

where M_r is the resilient modulus, σ_d is the cyclic deviator stress $(\sigma_1-\sigma_3)$, ε_a is the resilient axial strain, σ_1 is the maximum principal stress, and σ_3 is the minimum principal stress (confining pressure). The definitions for cyclic deviator stress σ_d and resilient axial strain ε_a are shown in Fig. 17.

Resilient modulus M_r depends on the number of cyclic loadings. In the early stages, the resilient axial strain decreases as the number of stress applications increases. However, the resilient strain will tend to stabilize after a sufficient number of cyclic loadings, and the resilient modulus at this time can be used to characterize the behavior of the materials.

Figure 18 shows the variation in elastic strain ε_e and accumulation plastic strain ε_p with an increase in the cyclic loading number. Both elastic strain ε_e and accumulation plastic strain ε_p tend to stabilize after 10,000 cyclic loadings. Furthermore, although some difference for ε_e or ε_p between the ferrum-lime stabilized soil and the hydrated-lime stabilized soil can be observed, it will become indistinct as the number of cyclic loading increases.

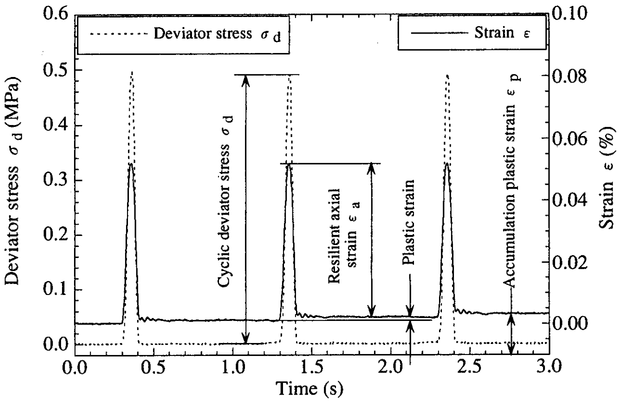

Fig. 17. Definition of resilient strain ε_a and plastic strain ε_p

The Resilient Modulus of Ferrum Lime Stabilized Soil

In tests, deviator stress σ_d and mean principal stress σ_m were modified to observe the dependence of the resilient modulus on the deviator stress and the mean principal stress.

In Fig. 19, the solid lines indicate the relationships between resilient modulus M_r and peak deviator stress σ_d for specimens with a 28-day curing time and a 7% ferrum lime content at peak mean principal stress levels of 98.1 kPa, 196.2 kPa, and 294.3 kPa. Resilient modulus M_r decreases with an increase in the deviator stress if the deviator stress is lower than 450 kPa. However, it may become unvarying or only show a tiny increase along with a continual increase in the deviator stress application. Subsequently, the variation in resilient modulus M_r with an increase in the mean principal stress can be noticed; the variation in resilient modulus M_r is not obvious when mean principal stress σ_m increases from 98.1 kPa to 196.2 kPa. M_r has a distinct increment, however, if mean principal stress σ_m increases from 196.2 kPa to 294.3 kPa. Based on this fact, resilient modulus M_r depends on both the deviator stress and the mean principal stress. All of the resilient modulus vs deviator stress curves are similar to a parabolic curve. The resilient modulus-stress relationship can be expressed by the equation for a family of parabolic curves as follows:

$$M_r=a+b\sigma_d+c\sigma_d^2+d\sigma_m^n \tag{12}$$

where M_r is the resilient modulus (MPa), σ_d is the deviator stress (kPa), σ_m is the mean principal stress (kPa), and a, b, c, d, n are experimental constants.

According to a suitable calculation, experimental constants a, b, c, d, and n can be determined as shown in Fig. 19. The fitted curves (dotted lines), regressed by Eq. (12), match the experimental data perfectly. Experience Eq. (12) has a practical usage for a design or an analysis when the ferrum lime stabilized soil is used as road base

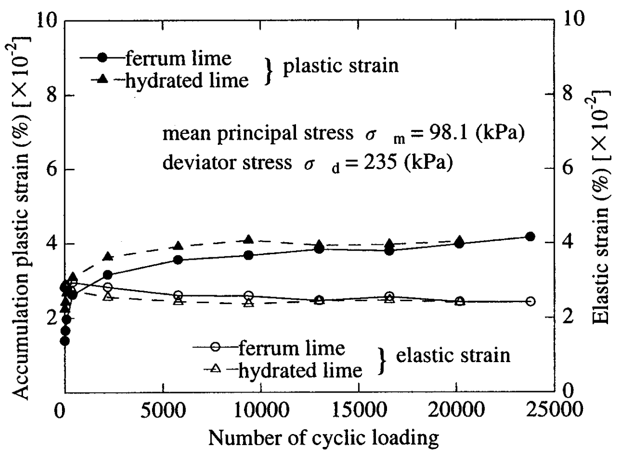

Fig. 18. Accumulation plastic strain and elastic strain plotted against number of cyclic loading

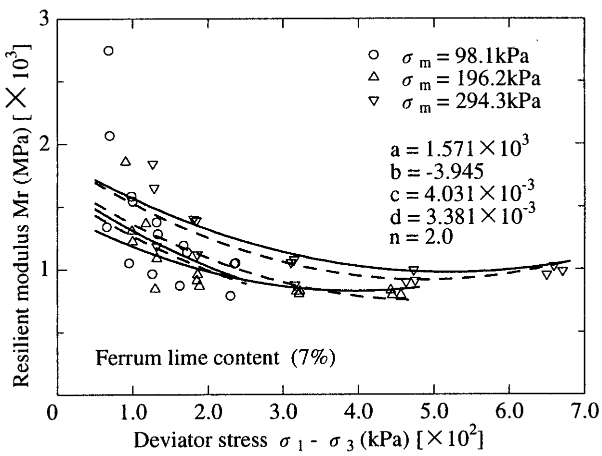

Fig. 19. Resilient modulus M_r versus deviator stress σ_d or mean principal stress σ_m

material.

Based on the results shown in Fig. 20, the dependency of resilient modulus M_r on the ferrum lime content tends to weaken with an increasing deviator stress. However, the resilient modulus may not depend on the ferrum lime content if the mean principal stress is kept at a higher level, as shown in Fig. 21. As a result, the dependency of the resilient modulus on the ferrum lime content is not strong except at a lower deviator stress level.

A comparison of the test results for specimens stabilized by ferrum lime and hydrated lime is presented in Figs. 22 and 23. The hydrated-lime stabilized soil shows a lower resilient modulus M_r as opposed to the ferrum-lime stabilized soil if deviator stress σ_d and mean principal stress σ_m are kept at lower levels. However, the resilient modulus M_r of the two types of stabilized soils may tend to be near each other with an increase in the deviator stress or the mean principal stress application. Based on these results, pavement stabilized by ferrum lime may show a lower elastic deformation than that stabilized by hydrated lime if the ferrum-lime stabilized soil is used as subbase or subgrade material, because the stress application is quite low in subbase or subgrade.

The Correlation between Dynamic Properties and Static Properties

In Fig. 24, measured resilient modulus M_r (solid lines) increases with an increase in unconfined compressive strength q_u if the mean principal stress is kept at σ_m=98.1 kPa. However, the dependence of resilient modulus M_r on unconfined compressive strength q_u tends to weaken with an increase in the deviator stress application. Furthermore, when examining the dependence of resilient modulus M_r on unconfined compressive strength q_u at mean principal stress σ_m=294.3 kPa, as shown in Fig. 25, the dependence of resilient modulus M_r on unconfined compressive strength q_u is not distinct. In the results, the resilient modulus of ferrum lime stabilized soil has a low dependency on the static compressive strength with a higher mean principal stress or deviator stress besides a lower deviator stress application.

Examining the correlation between resilient modulus M_r and the unconfined compressive strength, together with the deviator stress application, the resilient modulus

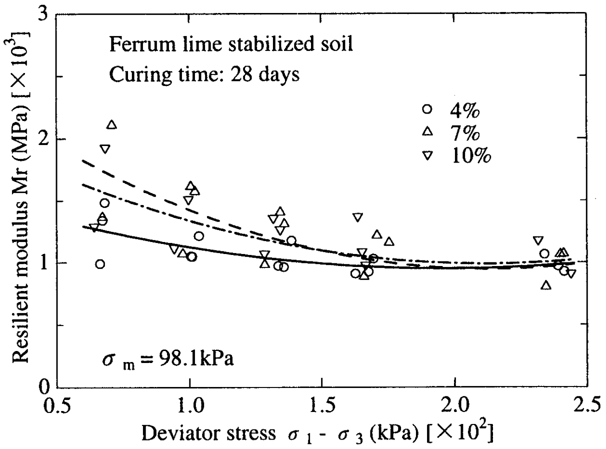

Fig. 20. Resilient modulus M_r versus deviator stress at mean principal stress σ_m=98.1 kPa

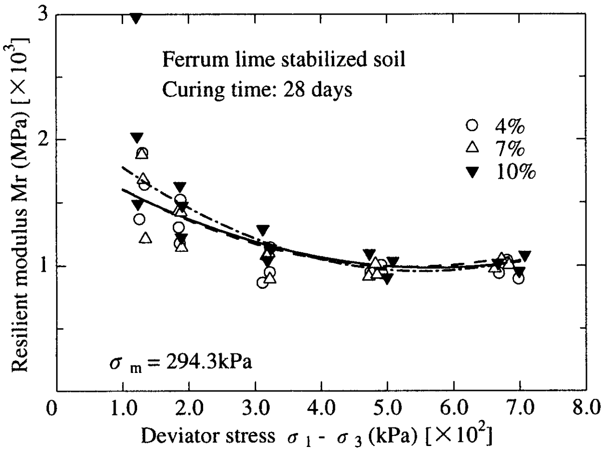

Fig. 21. Resilient modulus M_r versus deviator stress at mean principal stress σ_m=294.3 kPa

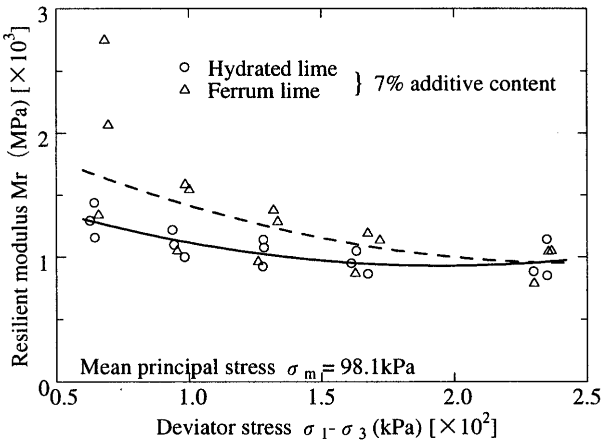

Fig. 22. Resilient modulus M_r versus deviator stress σ_d

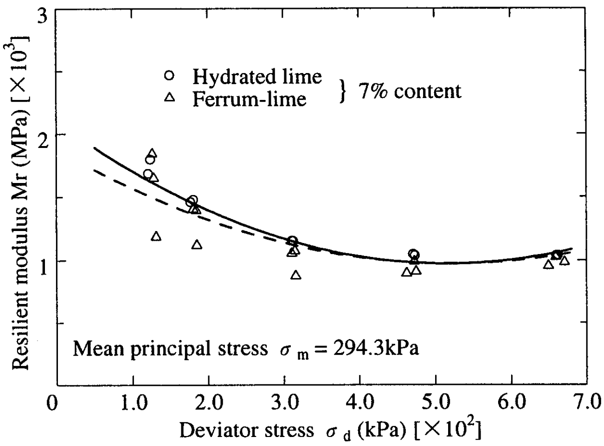

Fig. 23. Resilient modulus M_r versus deviator stress σ_d

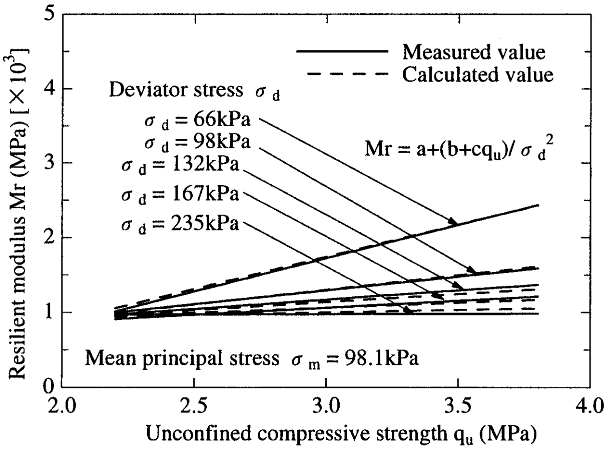

Fig. 24. Resilient modulus M_r versus unconfined compressive strength q_u at mean principal stress σ_m=98.1 kPa

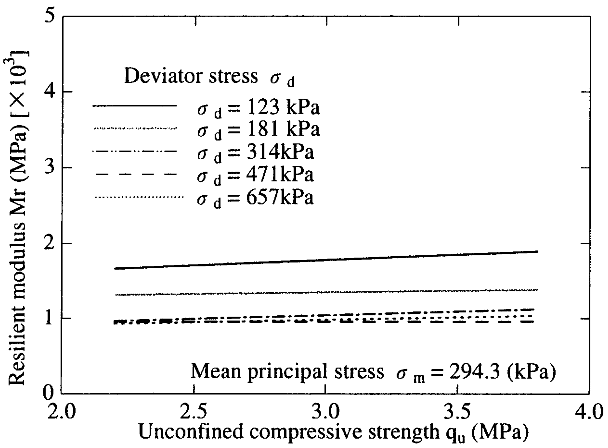

Fig. 25. Resilient modulus M_r versus unconfined compressive strength q_u at mean principal stress σ_m=294.3 kPa

M_r varies linearly with an increase in unconfined compressive strength q_u while keeping the deviator stress at a certain level. Based on the above characteristic, the relationship between resilient modulus M_r and unconfined compressive strength q_u can be described by a linear equation. Thereby, when the regressive equation as Eq. (13) is used to predict resilient modulus M_r at a lower deviator stress application, the predicting values (dotted lines) coincide fairly well with the measured lines (solid lines), as shown in Fig. 24.

$$M_r = a + \frac{(b + cq_u)}{\sigma_d^2} \tag{13}$$

where M_r is the resilient modulus, q_u is the unconfined compressive strength, σ_d is the deviator stress, and a, b, and c are the test parameters.

Since there is an approximate linear relation between unconfined compressive strength q_u and static modulus E_{50}, putting E_{50} into expression (13) instead of q_u yields a similar expression.

THE EVALUATION OF FERRUM LIME STABILIZED SOIL USED AS ROAD BASE MATERIAL

Improving road base with a composite material can raise the pavement life due to the improved resistibility to cracks and the decrement of compressive strain on top of the subgrade. Based on the above-mentioned test results and examinations, the compressive properties of stabilized soil can be promoted by adding ferric oxide to the hydrated lime. Pavement stabilized by ferrum lime may have a lower compressive strain than that stabilized by hydrated lime if the stabilized soil is used as road base material. For flexural properties which are important for upper road base materials, the differences between flexural strength σ_d and fracture surface energy γ_s for ferrum-lime and hydrated-lime stabilized soils are not clear. Therefore, the ferrum-lime stabilized soil would have almost the same resistibility to cracks as the hydrated-lime stabilized soil. Since the ferrum-lime stabilized soil has a greater resilient modulus than the hydrated-lime stabilized soil when the stress application is at a lower level, the former may be better than the latter in limiting pavement deflection. According to the above inferences, ferrum-lime stabilized soil has better durability than hydrated-lime stabilized soil when it is used as road base material.

CONCLUSIONS

The study presented in this paper was based on results from a series of laboratory tests on ferrum-lime stabilized soil. According to these results, the following conclusions were obtained.

(1) The unconfined compressive strength of ferrum-lime stabilized soil increases with an increase in the ferrum-lime content from 4% to 7%. However, the increment is insignificant if the ferrum lime content is increased from 7% to 10%. As a result, it is unnecessary to use a ferrum lime content over 7%.

(2) Although the flexural strength may increase with an increase in the ferrum lime content, fracture surface energy γ_s, related to the resistance to cracks, seems to have a low dependence on the ferrum lime content or the flexural strength. However, it clearly may depend on the flexural failure deflection.

(3) The resilient modulus of ferrum-lime stabilized soil depends on both the deviator stress and the mean principal stress. The resilient modulus-deviator stress relationship of ferrum-lime stabilized soil appears to be nonlinear in keeping a certain mean principal stress. This relationship could be regressed with the equation for a family of parabolic curves. The dependence of the resilient modulus on the ferrum lime content is not strong and has a lower deviator stress application.

(4) In examining the relation between the resilient modulus and the static compressive strength, the resilient modulus increases with an increase in the compressive strength if the deviator stress application is kept at a low-

er level. However, the dependence of the resilient modulus on the static compressive strength may tend to weaken when increasing the deviator stress or the mean principal stress application.

(5) In comparing ferrum-lime stabilized soil with hydrated-lime stabilized soil, the former shows better compressive properties than the latter. Summarizing the above results, ferrum lime stabilized soil may have better durability in comparison to hydrated-lime stabilized soil as it is used as road base material.

ACKNOWLEDGMENTS

The authors wish to thank Dr. Mamoru Mimura, Associate Professor, DPRI, Kyoto University for his invaluable suggestions in preparing this paper. We are also grateful to Mr. Takao Yano, Technician, Department of Civil Engineering, Kyoto University for his assistance in conducting the dynamic triaxial cyclic tests and the fracture surface measuring with the Laser Roughness Measurer. In addition, Mr. Ryohei Okada, former Graduate Student, Department of Civil Engineering, Kyoto University, and Mr. Masahiro I, Research Student, DPRI, Kyoto University are thanked for their assistance with the laboratory tests.

REFERENCES

1) Abe, Y. (1993): "Development of ferrum-lime stabilized soil," Pavement, Vol. 28, No. 9, pp. 16–21 (in Japanese).
2) Blight, G. E. (1973): "Fracture of pavement materials," Proc. of the American Society of Civil Engineers, Vol. 99, No. TE4, pp. 801–819.
3) Boniface, C. and Obi, A. (1972): "Soil-cement bases under thin bituminous surfacing," Proc. of the American Society of Civil Engineers, Vol. 98, No. TE2, pp. 167–176.
4) Brown, S. F. (1996): "Soil mechanics in pavement engineering," Gêotechnique, Vol. 46, No. 3, pp. 383–426.
5) George, K. P. (1970): "Theory of brittle fracture applied to soil cement," Proc. of the American Society of Civil Engineers, Vol. 96, No. SM3, pp. 991–1010.
6) Jin, M. S., Lee, K. W. K. and Kovacs, W. D. (1994): "Seasonal variation of resilient modulus of subgrade soils," J. of Transportation Engrg., ASCE, Vol. 120, No. 4, pp. 603–616.
7) Khedr, A. S. (1986): "Deformation mechanism in asphaltic concrete," J. of Transportation Engrg., ASCE, Vol. 112, No. 1, pp. 29–45.
8) Lee, S. W. and Fishman, K. L. (1993): "Waste products as highway materials in flexible pavement system," J. of Transportation Engrg., ASCE, Vol. 119, No. 3, pp. 433–449.
9) Mamlouk, M. S. and Wood, L. E. (1981): "Characterization of asphalt emulsion treated bases," Proc. of the American Society of Civil Engineers, Vol. 107, No. TE2, pp. 183–196.
10) Matsuo, S. and Kamon, M. (1977): "Improvement of engineering properties of soft clay by addition of iron ions," J. of the Society of Materials Science, Japan, Vol. 26, No. 290, pp. 1034–1040 (in Japanese).
11) Nishi, K. (1981): "Mechanical properties of flexible pavement," The Recent Problems and New Techniques about Pavement, Lecture Text in S53, Kansai Branch of Society of Japan Civil Engineers, pp. 3–33 (in Japanese).
12) Nishi, K. and Yoshida, N. (1993): "Rutting analysis of asphalt pavement with circular loaded test," Construction Engrg. Research Report, No. 35, pp. 159–168 (in Japanese).
13) Sauer, E. K. and Weimer, N. F. (1978): "Deformation of lime modified clay after freeze-thaw," Proc. of the American Society of Civil Engineers, Vol. 104, No. TE2, pp. 201–212.
14) Thompson, M. R. and Robnett, Q. L. (1979): "Resilient properties of subgrade soils," Proc. of the American Society of Civil Engineers, Vol. 105, No. TE1, pp. 71–89.
15) Zaman, M., Chen, D. H. and Laguros, J. (1994): "Resilient moduli of granular materials," J. of Transportation Engrg., ASCE, Vol. 120, No. 6, pp. 967–988.